Optical and electro-optical properties of lithium thallium tartrate monohydrate

1989 J. Phys.: Condens. Matter 1 6441

(http://iopscience.iop.org/0953-8984/1/36/012)

J. Phys.: Condens. Matter 1 (1989) 6441–6452. Printed in the UK

Optical and electro-optical properties of lithium thallium tartrate monohydrate

Y Zhu†‡, P Günter†, J Fousek†§ and B Březina‖

† Institute of Quantum Electronics, Swiss Federal Institute of Technology, ETH Hönggerberg, CH-8093 Zürich, Switzerland

‖ Institute of Physics, Czechoslovak Academy of Sciences, Na Slovance 2, CS-18040 Prague, Czechoslovakia

Received 17 January 1989

Abstract. The electro-optic coefficients r_{ij} and birefringence components of lithium thallium tartrate (LTT) single crystals have been measured in the 5–300 K temperature range, as also have the refractive indices at room temperature. The coefficients r_{41}, r_a and r_b behave in an anomalous way in the vicinity of $T_c \approx 12$ K where LTT undergoes a phase transition; below T_c, r_{41} reaches a high value of 500 pm V^{-1}. Their behaviour can be explained by considering the transition to be of a proper ferroelectric–proper ferroelastic nature, triggered by a balance between the values of clamped susceptibility, elastic stiffness and piezoelectric coefficient, as suggested earlier. A model of built-in strain is employed to interpret the existence of the symmetry-breaking coefficients r_a and r_b in the symmetric phase. The measured optical properties are used to re-examine the possibility of distinguishing domains in polarised light.

1. Introduction

Single crystals of lithium thallium tartrate (LTT) ($LiTlC_4H_4O_6.4H_2O$) are of orthorhombic $P2_12_12_1$ symmetry at room temperature (Kay 1978) and transform into a ferroelectric phase at about 12 K (Matthias and Hulm 1951). The latter is manifested by the presence of spontaneous polarisation along the orthorhombic a axis and by the Curie–Weiss behaviour of the permittivity ε_1 (Matthias and Hulm 1951, Fousek *et al* 1970). The very existence of a dielectric anomaly can be considered an indication that the ferroelectric transition is not of an improper nature. Although direct structural data are not available it may be therefore assumed that the instability occurs at the Brillouin zone centre, owing to a B_3 symmetry mode, leading to the monoclinic ordered phase of symmetry $P2_1$.

Since both polarisation P_1 and shear deformation S_4 transform according to the B_3 representation, their coupling affects the stress-free permittivity ε_1^T exhibiting Curie–Weiss behaviour. For the stress-free susceptibility χ_1^T the following expression is valid:

‡ On leave of absence from the Institute of Physics, Chinese Academy of Sciences, Beijing, People's Republic of China.

§ On leave of absence from the Institute of Physics, Czechoslovak Academy of Sciences, Prague, Czechoslovakia.

0953-8984/89/366441 + 12 $02.50

$$(\chi_1^T)^{-1} = (\chi_1^S)^{-1} - a_{14}^2/c_{44}^P \tag{1.1}$$

where the superscript S denotes the clamped value, a_{14} is the piezoelectric stress coefficient and c_{44}^P is the elastic stiffness at constant polarisation. The instability is reached at a temperature T_c at which $(\chi_1^T)^{-1}$ approaches zero. In this respect, LTT may be compared with two other ferroelectrics whose anomalous χ^T component is given by an analogous relation: potassium dihydrogen phosphate (KDP) (P_3 couples to S_6) and lithium ammonium tartrate (LAT) (P_2 couples to S_5) (Maeda and Ikeda 1977, Sawada *et al* 1977). It is known that these two compounds behave in a very different way. In KDP the source of instability is dielectric in that $(\chi_1^T)^{-1}$ approaches zero owing to the temperature dependence of the clamped susceptibility χ^S, while c^P and a are constant (Baumgartner 1951). In LAT the driving mechanism of the transition is primarily elastic (Sawada *et al* 1977) since $c^P(T)$ is the source of Curie–Weiss behaviour while χ^S and a are temperature independent.

It was discovered by Sawaguchi and Cross (1971) that in LTT the way to instability, on cooling, is rather unexpected. The clamped susceptibility at room temperature does not exceed 20 and increases slowly by a factor of only about 2.5 between 300 K and T_c. However, both further quantities a_{14} and c_{44}^P on the right-hand side of equation (1.1) also depend slightly on temperature in such a way that $(\chi_1^T)^{-1}$ approaches zero at T_c and a Curie–Weiss behaviour results. We may, therefore, classify LTT as a case intermediate between KDP and LAT. All three materials undergo a proper ferroelectric–proper ferroelastic transition but the normal soft-mode eigenvectors are different. Since in LTT the coupling constant a between P and S depends on T, the character of this eigenvector can also be expected to change with temperature.

More recently, Gerbaux *et al* (1985) reported the existence of an infrared-active vibrational mode at 21 cm^{-1} whose frequency decreased to 11 cm^{-1} near T_c. A more detailed investigation using submillimetre spectroscopy (Volkov *et al* 1986) revealed that this mode's contribution to ε_1 is about 5 at room temperature and increases on approaching T_c where it reaches the maximum value of about 19. Neither the frequency nor the strength of this oscillator show critical behaviour; in addition, the behaviour of its damping is typical of a hard mode. These facts fully support the conclusion of Sawaguchi and Cross (1971) that the clamped susceptibility is non-critical and that the balance between χ_1^S, c_{44}^P and a_{14} leads to the phase transition.

All the above discussion is based on the assumption that at $T_c = 12$ K the symmetry of LTT does in fact change. As already mentioned, no direct x-ray evidence is available. One symmetry-breaking quantity, the polarisation P_s, was actually found to reach zero at T_c by several researchers working with crystals from two independent sources (Fousek *et al* 1970, Sawaguchi and Cross 1972, Abe *et al* 1974). Other investigators (Novik *et al* 1982) claim to have observed a non-zero pyroelectric signal which decreases with increasing T but extending some 40 K above T_c whose integration, however, gives only a very low value of about 2×10^{-5} C m^{-2} at 50 K. In this connection the study of Khaller *et al* (1988) of the Raman spectra of LTT should also be mentioned. They reached the conclusion that at T_c the structure of the unit cell as a whole does not change; in this sense the phase transition 'appears to be isostructural and smeared out'.

The LTT single crystals grown from water solution (Březina *et al* 1970) are transparent, water clear and free of visible defects. The quality of these crystals was found suitable even for a Brillouin experiment in which the elastic stiffness components were determined (Pavel *et al* 1988). It is therefore surprising that almost no data on optical and electro-optical properties are available, in particular in KDP because the electro-optical

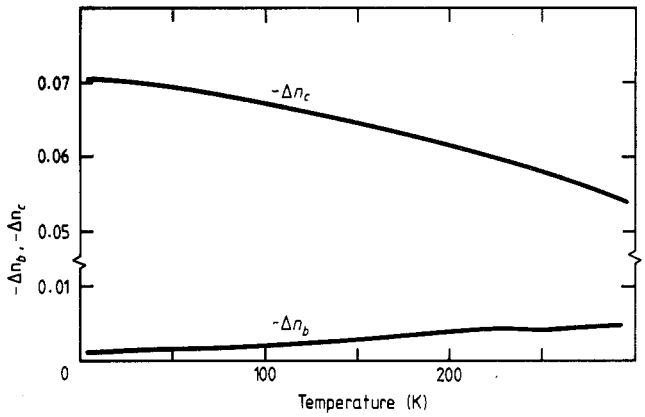

Figure 1. The temperature dependences of birefringence components.

behaviour provides a significant additional argument for the source of dielectric instability. The experiment with LTT crystals is, of course, more elaborate because of the He temperature range. It is the aim of the present paper to fill this gap partially by determining the principal refractive indices and obtaining basic information on the temperature dependence of the birefringence components. In particular, we wish to investigate the linear electro-optical effect in LTT connected with the field applied along the prospective polar axis a and to compare the possible electro-optical behaviour of the three categories of materials mentioned. Finally, we wish to verify whether the smearing effects referred to manifest themselves in the optical properties.

2. Basic optical properties

Crystal plates oriented normal to the orthorhombic a, b and c axes were used for the measurements of refractive indices and birefringence components. The former were determined using an Abbé refractometer. For $T = 22$ °C and $\lambda = 633$ nm, we found that

$$n_a = 1.659 \pm 0.001$$

$$n_b = 1.713 \pm 0.001$$

$$n_c = 1.654 \pm 0.001.$$

The complete dispersion curves were not measured. However, experiments using a spindle stage revealed a crossing of the refractive indices n_a and n_c at a wavelength of 589 nm. Thus at 589 nm and at 22 °C the crystal becomes effectively uniaxial, with the optical axis oriented along the crystallographic axis b.

A Zeiss Ehringhaus-type calcite compensator was employed to measure the birefringence. Figure 1 shows the temperature dependence of $\Delta n_b = n_c - n_a$ and $\Delta n_c = n_a - n_b$; for $\lambda = 633$ nm, both are negative. Their temperature coefficients differ in sign; $\mathrm{d}(\Delta n_b)/\mathrm{d}T > 0$ while $\mathrm{d}(\Delta n_c)/\mathrm{d}T < 0$.

The measurement precision available made it impossible to evaluate spontaneous birefringence values below T_c defined as $\delta_s[\Delta n_i(T)] = \Delta n_i(T) - \Delta n_i$ (extrapolated to T from above T_c). However, an inspection of the data below T_c shows that $\delta_s(\Delta n_b) > 0$ and also $\delta_s(\Delta n_c) > 0$.

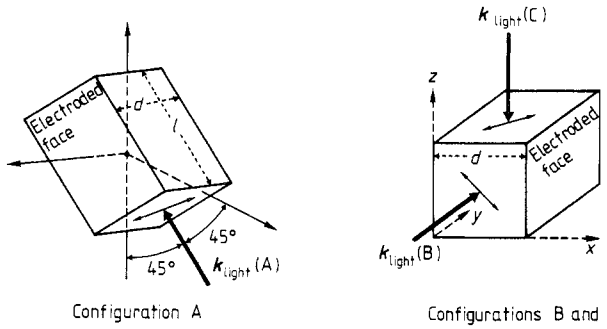

Figure 2. The sample geometries used to determine the half-wave voltage: configuration A was used for the measurement of r_{41}, configuration B for the measurement of r_b and configuration C for the measurement of r_c.

3. Electro-optical properties

Electro-optical behaviour was studied using the modulation method described by Günter (1976). In all cases the geometry corresponded to a transverse effect and the external field directed along the orthorhombic axis *a* since this will become the ferroelectric axis. The measuring AC field E_1 at a frequency of 10 kHz was applied by means of gold evaporated electrodes covering the (100) faces of the samples completely. With respect to the piezoelectric resonance frequencies of LTT (Sawaguchi and Cross 1971), our measuring frequency $f = 10$ kHz is low enough to ensure stress-free conditions for samples used in this study. An exchange gas helium cryostat (type CF 200 Oxford continuous-flow cryostat) was used to change the sample temperature and to keep it constant during the measurement).

In the parent orthorhombic phase and for $E = E_1$, only the electro-optic coefficient r_{41} is active. To determine this, we chose the geometry A shown in figure 2. The velocities of light propagating along [0 1 1] are determined by the refractive indices

$$n_{[100]} = n_a$$

$$n_{[1\bar{1}0]} = (\sqrt{2}n_b n_c/\sqrt{n_b^2 + n_c^2})\,[1 + n_b^2 n_c^2 r_{41} E_1/(n_b^2 + n_c^2)]$$

where the subscripts in square brackets indicate the polarisation of the light wave. From this the following expression for the half-wave voltage can be deduced:

$$V_{\lambda/2}(A, T > T_c) = [(n_b^2 + n_c^2)/2n_b^2 n_c^2]^{3/2}(\lambda/r_{41})(d/l) \tag{3.1}$$

where d is the electrode spacing and l denotes the light path in the sample.

In the low-symmetry phase (assumed here to be of symmetry 2) the polar axis is usually identified with the crystallographic axis *b*. However, to make use of a unified coordinate system for both phases, we keep denoting the ferroelectric axis as *a*. Then the field E_1 activates the following electro-optic coefficients: r_{11}, r_{21}, r_{31} and r_{41}. All of these influence, in the A geometry, the half-wave voltage for which we obtain the formula

$$V_{\lambda/2}(A, T < T_c) = \{\tfrac{1}{2}(r_{21} + r_{31} + 2r_{41})[2n_b^2 n_c^2/(n_b^2 + n_c^2)]^{3/2} - r_{11}n_a^3\}^{-1}\,\lambda(d/l). \tag{3.2}$$

For graphical representation of the results in the A geometry it is practical to introduce

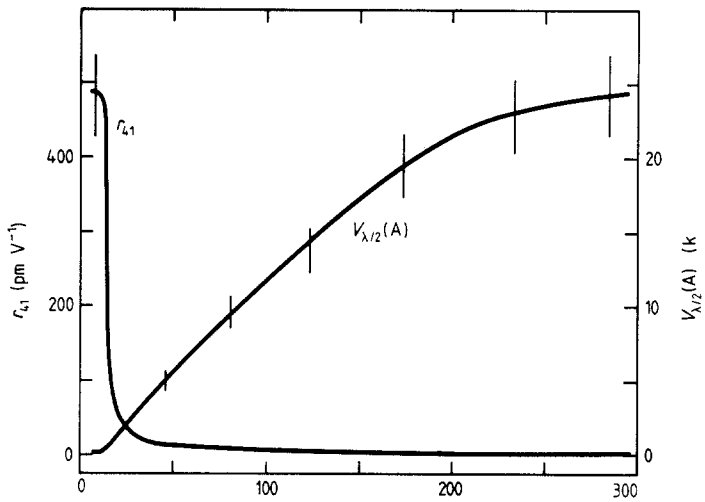

Figure 3. The same quantities as in figure 4 (below) over a wide temperature range.

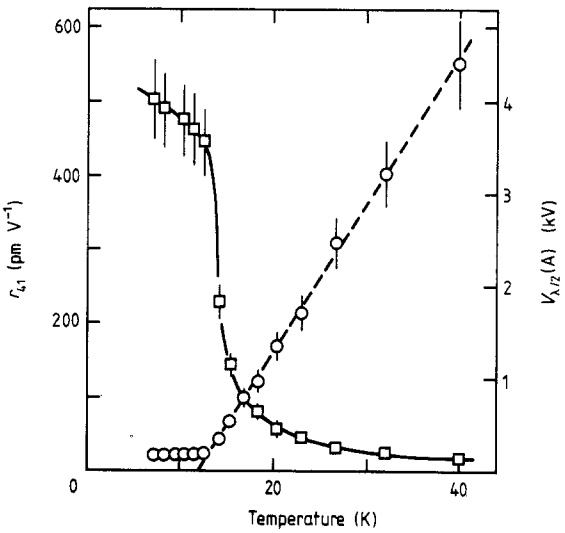

Figure 4. The temperature dependences of the half-wave voltage $V_{\lambda/2}(A)$ (○) and of r_{41} (□) (the latter is denoted as $r_{ef}(A)$ below T_c) close to T_c.

an effective electro-optic coefficient $r_{ef}(A)$ by putting the term in braces in the last expression equal to

$$[(n_b^2 + n_c^2)/2n_b^2n_c^2]^{3/2}\,[1/r_{ef}(A)]. \tag{3.3}$$

Figure 3 shows the temperature dependence of $V_{\lambda/2}(A)$ over a wide range of temperatures. These data were obtained with a sample of dimensions $d = 2.42$ mm, $l = 4.71$ mm and 2.9 mm along the [100], [011] and [01$\bar{1}$] directions, respectively. We observe a quasi-linear decrease with decreasing T; however, far above T_c a tendency to saturation is evident. In the same figure, $r_{41}(T)$ is plotted, which becomes $r_{ef}(A)$ below T_c. Figure 4 provides a more detailed picture of the behaviour near T_c. Assuming a Curie–Weiss law just above T_c, one obtains by extrapolation $T_c = 12$ K, in good agreement with the results of previous investigators.

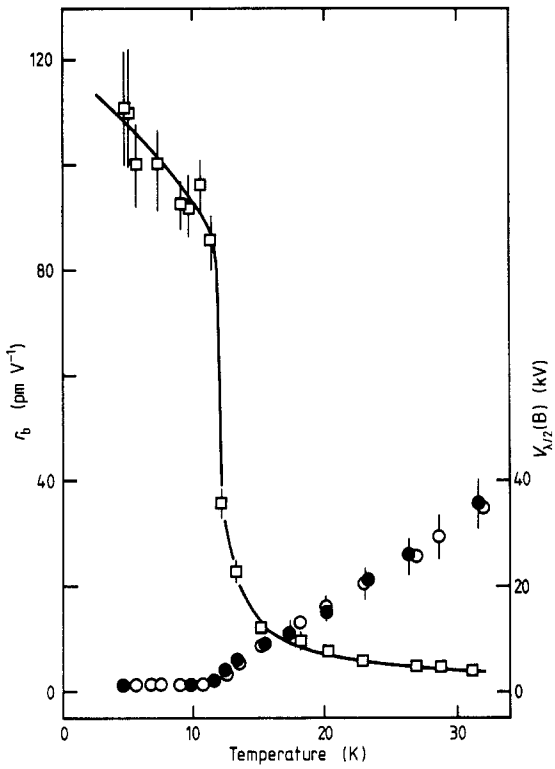

Figure 5. The temperature dependences of the half-wave voltage $V_{\lambda/2}$(B) for $E_{bias} = 0$ V cm^{-1} (○) and for $E_{bias} =$ 180 V cm^{-1} (●) and of r_b (□).

To determine independent information about the r_{11}, r_{21} and r_{31} coefficients in the monoclinic phase, two other geometries B and C for the transverse effect were used; these are shown schematically in figure 2. For configuration B the half-wave voltage is

$$V_{\lambda/2}(\mathrm{B}) = (\lambda/n_a^3 r_b)(d/l)$$

with

$$r_b = r_{11} - (n_c/n_a)^3 r_{31}$$

while, for configuration C,

$$V_{\lambda/2}(\mathrm{C}) = (\lambda/n_a^3 r_c)(d/l)$$

with

$$r_c = r_{11} - (n_b/n_a)^3 r_{21}.$$

The experimental data were obtained for a sample with dimensions $d = 3.1$ mm, 3.57 mm and 3.4 mm along a, b and c, respectively.

For the last two cases the results are shown in figures 5 and 6. Below T_c the values of $r_b \simeq 100$ pm V^{-1} and $r_c \simeq 40$ pm V^{-1} are considerably smaller than that of $r_{ef}(\mathrm{A}) \simeq$ 500 pm V^{-1}. Here we have in mind absolute values since the AC method used in this study did not allow us to determine the signs. Somewhat surprisingly, all three coefficients have similar temperature dependences.

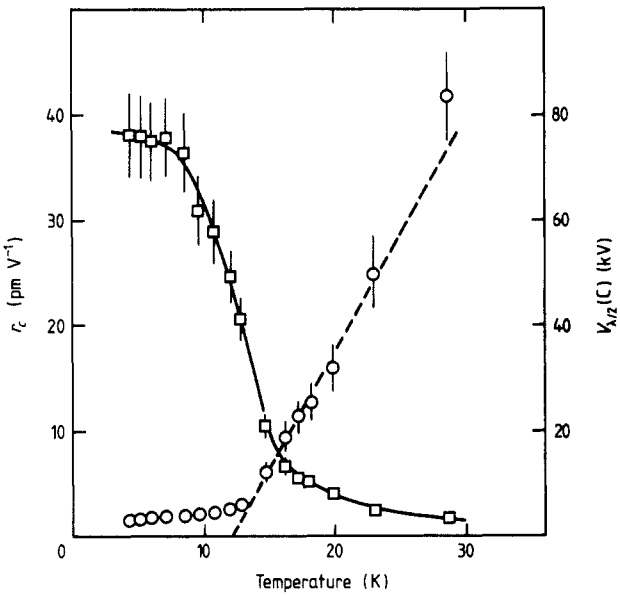

Figure 6. The temperature dependences of the half-wave voltage $V_{\lambda/2}(C)$ (○) and of r_c (□).

4. Discussion

The broad temperature range in which birefringence has been measured, i.e. some 280 K above T_c, is unique and these data, fitted by a polynomial, would provide an excellent basis for the precise determination of spontaneous birefringence or of possible precursor effects. However, data below T_c with a higher relative accuracy will have to be obtained to fulfil this task. It will be instructive for the following discussion of electro-optical properties to analyse briefly the basic spontaneous optical effects in the three classes of materials mentioned in § 1. These effects can be described by spontaneous changes $\delta_s B_{ij}$ where the impermittivity $B_{ij} = \varepsilon_0 dE_i/dD_j$ defines the optical index ellipsoid $B_{ij}x_i x_j = 1$. In all the above-mentioned types of proper ferroelectric–proper ferroelastic transition it is an off-diagonal component of B_{ij} which couples linearly (Fousek and Petzelt 1979) to the order parameter: B_{12} for KDP, B_{13} for LAT and B_{23} for LTT. Their spontaneous changes are manifested by spontaneous birefringence in KDP:

$$\delta_s(\Delta n_{12}) = n_a^3 \, \delta_s B_{12} \tag{4.1}$$

(measured in a system rotated by 45° around z) and by spontaneous indicatrix rotations in the other two cases: about the b axis in LAT,

$$\tan(2\beta) = 2[n_a^2 n_c^2/(n_a^2 - n_c^2)] \, \delta_s \, B_{13} \tag{4.2}$$

and, about the a axis in LTT,

$$\tan(2\alpha) = 2[n_c^2 n_b^2/(n_c^2 - n_b^2)] \, \delta_s \, B_{23}. \tag{4.3}$$

The last three equations make it possible in principle to determine $\delta_s B$ experimentally.

This then may be related to other spontaneous quantities. Omitting all subscripts, we can write for any of the three cases

$$\delta_s B = p^P S + f^S P. \tag{4.4}$$

Here the elasto-optic coefficient p^P can be regarded as essentially independent of T. The same is true for the clamped polarisation optical coefficient f^S, provided that P is unambiguously defined by the same ionic shifts whether they occur spontaneously below T_c or are field induced above T_c. We shall assume this to be the case.

For KDP-type behaviour, we can now easily deduce that

$$\delta_s B(T) = f^T P_s(T) \tag{4.5a}$$

where the stress-free coefficient f^T is also constant. Alternatively, the following equation holds (Fousek and Petzelt 1979):

$$\delta_s B(T) = p^E(T_c) S_s(T) \tag{4.5b}$$

where p^E is T dependent but remains finite at T_c. For LAT-type properties, these relations change to

$$\delta_s B(T) = p^E S_s(T) \tag{4.6a}$$

or

$$\delta_s B(T) = r(T_c) P_s(T). \tag{4.6b}$$

For LTT, $\delta_s B$ would be given by equation (4.4) where one of the S_s and P_s quantities could be eliminated by the relation $P_s = -(c^P/a)S_s$. Here, however, unlike the preceding case, c^P/a is T dependent (Sawaguchi and Cross 1971) and would have to be extrapolated from the parent phase:

$$\delta_s B(T) = [f^S - (p^P a/c^P)(T)] P_s(T) \tag{4.7a}$$

or

$$\delta_s B(T) = [p^P - (f^S c^P/a)(T) S_s(T). \tag{4.7b}$$

In the present paper the rotation given by equation (4.3) and consquently the value and temperature dependences of $\delta_s B_{23}$ were not determined but we may use the same formalism to discuss the known electro-optical properties. The electro-optic coefficient connected with off-diagonal impermittivity coupled to the order parameter is simply obtained by differentiating equation (4.4). Thus the clamped electro-optic coefficient is given by

$$r^S = f^S \chi^S \tag{4.8}$$

and its temperature dependence in the parent phase always copies that of χ^S. For stress-free conditions,

$$r = f\chi^T = (f^S - p^P a/c^P)[(\chi^S)^{-1} - a^2/c^P]^{-1}. \tag{4.9}$$

For KDP-type behaviour, f is constant and r follows the Curie–Weiss law of χ^T. More

complicated behaviour is possible for elastic instability as in LAT. There $c^P = \beta_0(T - T_0)$, $\beta_0 > 0$; the transition occurs at

$$T_c = T_0 + \chi^S a^2/\beta_0$$

and the stress-free susceptibility takes the form

$$\chi^T = \chi^S + C/(T - T_c)$$

with $C = \chi^S(T_c - T_0)$. Now equation (4.9) reads

$$r = [f^S - p^P a/\beta_0(T - T_0)][\chi^S + C/(T - T_c)]. \tag{4.10}$$

We get a divergence at T_c but not a simple Curie–Weiss behaviour above T_c. Numerical estimations show that in practice, whatever the signs of f^S, p^P and a might be, the term $f^S - p^P a/\beta_0(T - T_0)$ in equation (4.10) never changes sign.

For LTT, equation (4.9) reads

$$r_{41} = f_{41}\chi_1^T = (f_{41}^S - p_{44}^P a_{41}/c_{44}^P)\chi_1^T \tag{4.11}$$

with χ_1^T given by equation (1.1).

This relation may be compared with the experimental data. From the work by Sawaguchi and Cross (1971) we take the stress-free susceptibility in the form

$$\chi_1^T = \varepsilon_0[8 + 1330/(T - T_c)] \tag{4.12}$$

and use our T_c-value of 12 K. From the same source, we calculated the temperature dependence of a_{41}/c_{44}^P shown in figure 7. Since the latter quantity does not depend critically on T, near T_c we expect to have an r_{41} Curie–Weiss behaviour, in agreement with the data in figure 4. Further, above T_c, as seen in figure 3, r_{41} departs considerably from the Curie–Weiss law. The temperature dependence of the numerator in equation (4.11) may be responsible for this. Unfortunately, experimental data for f_{41}^S and p_{44}^P are not available. However, choosing a reasonable value for f_{41}^S of about 1.2×10^{-2} m^2 C^{-1}, we find that $p_{44}^P \simeq 4.3 \times 10^{-2}$ and, taking $p_{44}^P a_{41}/c_{44}^P > 0$, we obtain an $r_{41}(T)$ curve which agrees well with that shown in figure 3 to within a 10% accuracy in a range of 250 K above T_c. This reasonable agreement cannot be considered as very significant and the chosen values of f_{41}^S and p_{44}^P as unambiguous since in such a wide range of temperatures the two latter quantities are unlikely to have constant values.

Below T_c, in the geometry used for the measurement of r_{41}, the half-wave voltage is determined by the effective coefficient $r_{ef}(A)$ defined by equations (3.2) and (3.3). Figure 4 shows that it reaches the value of 500 pm V^{-1} in the range 4.5–11 K; this value is well above the average of known electro-optic coefficients.

We now turn to the results obtained for r_a and r_b (figures 5 and 6). Below T_c, these coefficients should arise from the quadratic electro-optical effect existing in the parent phase, biased by the presence of P_s:

$$r_i = f_i^T \chi_i^T = 2M_{i,ef} P_s \chi_1^T. \tag{4.13}$$

Here $M_{i,ef}$ describes the quadratic polarisation optical effect in the B ($i = b$) and C ($i = c$) geometry. This is a situation well known in ferroelectrics with a centrosymmetric para-electric phase (Fousek 1987). In the mean-field approximation for proper ferroelectrics, $\chi_1^T \sim (T_c - T)^{-1}$ and $P_s \sim (T_c - T)^{1/2}$; therefore, since M is roughly constant, r_i should increase when T_c is approached from below and should drop to zero above T_c. Neither of these predictions is fulfilled for LTT, as shown by figures 5 and 6. The behaviour

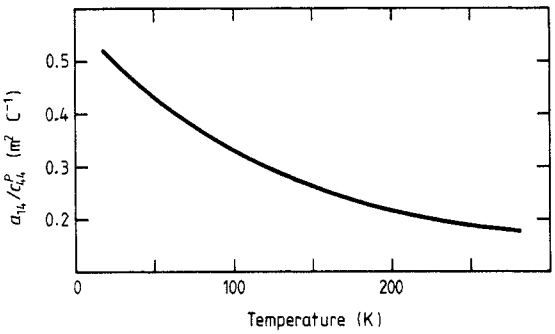

Figure 7. The ratio a_{14}/c_{44}^P as a function of temperature, determined using the data of Sawaguchi and Cross (1971).

below T_c, however, does not contradict equation (4.13); in LTT the susceptibility below T_c is roughly constant (Fousek *et al* 1970, Sawaguchi and Cross 1971, Novik *et al* 1982) for reasons not yet understood. Thus, $r_a(T)$ and $r_b(T)$ are mainly determined by $P_s(T)$ which shows a slight increase with decreasing T.

Above T_c the symmetry requires that $r_b = r_c = 0$. Instead, we observe a tail extending over at least 20 K above T_c. An external field of 0.18 kV cm^{-1} has almost no influence. We suggest the following mechanism to interpret this behaviour.

In the relation

$$P_1 = e_{14}S_4 + \chi_1^S E_1 \tag{4.14}$$

the piezoelectric strain coefficient e_{14} can be written as

$$e_{14} = a_{14}\chi_1^S. \tag{4.15}$$

Sawaguchi and Cross (1972) observed off-centre ferroelectric hysteresis loops in LTT and suggested the presence of an internal strain built into the samples owing to unspecified defects. According to equation (4.14) this strain brings about an unswitchable polarisation P_1^{int}. Since neither a_{14} nor χ_1^S changes critically at the transition, e_{14} and P_1^{int} will not be any pronounced functions of T near T_c. In keeping with equation (4.13), non-zero coefficients r_b and r_c are now induced, increasing in a Curie–Weiss manner (cf figures 5 and 6) as one approaches T_c from above, owing to χ_1^T given by equation (4.12). We may estimate the value of S_4^{int} required by this model. Since P_1^{int} must be much larger than polarisation induced by an applied field $E_1^{\text{ext}} = 180$ V cm^{-1}, the following inequality must hold: $a_{14}\chi_1^S S_4^{\text{int}} \gg \chi_1^S E_1^{\text{ext}}$, which results in $S_4^{\text{int}} \geqslant 10^{-4}$. This explanation is consistent even with the observations of Novik *et al* (1982) that a pyroelectric effect survives high above T_c; the product $a_{14}\chi_1^S$ decreases with increasing T, leading to $\mathrm{d}P_1^{\text{int}}/\mathrm{d}T \neq 0$.

As the final remark, we wish to consider the possibility of distinguishing ferroelectric domains in LTT in a polarised light. The only experimental attempt to observe the domains reported so far was negative (Fousek *et al* 1970). Now all data are available to re-estimate the angle between extinction positions in the two domains for light propagating along the a axis. This angle consists of two contributions. One is due to indicatrix rotation by the angle α given by equations (4.3) and (4.7*a*). Numerically we now obtain $\alpha = 7'$. The second contribution comes from the spontaneous value of S_4 since two neighbouring domains must be rotated by this angle to meet along a domain wall. The estimation based on the equation $S_4 = a_{14}/c_{44}^P$ gives approximately $2'$. Thus, direct visibility of domains due to difference in extinction positions is not possible with a conventional optical set-up; this does not mean, however, that the domain walls themselves could not produce some contrast, as known in other ferroelastics.

5. Conclusions

The refractive indices of LTT single crystals all lie between 1.65 and 1.71; n_a and n_c dispersion curves cross at 589 nm, making the crystal effectively uniaxial at this wavelength. The temperature dependences of birefringence components were measured in the range 5–300 K, showing that $d(\Delta n_b)/dT > 0$ while $d(\Delta n_c)/dT < 0$. Spontaneous changes in Δn occurring because of the phase transition are both positive.

Spontaneous changes in optical impermittivities at phase transitions which are simultaneously both proper ferroelectric and proper ferroelastic are analysed for three classes of materials differing in their sources of lattice instability. The same formulism can be used to treat their electro-optical properties. The linear electro-optical effect in LTT crystals was studied in detail. To the present authors' knowledge, the results of these measurements represent the first data on electro-optical behaviour at very low temperatures. In the range 5–12 K, i.e. below the phase transition temperature, the electro-optic coefficient r_{41} reaches a value of 500×10^{-12} m V^{-1} which is well above the average of the known electro-optical crystals. Its temperature dependence in the symmetric phase exhibits a Curie–Weiss-type behaviour some 50 K above T_c and shows a tendency to saturate at higher temperatures. Below T_c a rather sharp increase in r_{41} is observed. This behaviour is consistent with earlier measurements of clamped susceptibility, elastic stiffness and piezoelectric coefficient which indicated that the lattice leading to the transition is due to slowly varying terms in the free-energy function rather than to critical behaviour of a dielectric or elastic nature.

Other effective electro-optic coefficients r_b and r_c reach the values of 100×10^{-12} m V^{-1} and 40×10^{-12} m V^{-1}, respectively, below T_c. By symmetry, they should be non-existent in the high-symmetry phase. Contrary to this, they decrease in a Curie–Weiss way and are measurable down to $T_c + 20$ K where they drop to units of a value of picometres per volt. This behaviour can be well explained by the presence of a built-in strain S_4 of the order of 10^{-4} which smears out the transition. Such a model is consistent with the presence of a small pyroelectric effect which extends into the para-electric phase but decreases with increasing temperature, reported earlier.

The measured optical properties are used to estimate the difference in the extinction positions of domains. A maximum value of only about 9′ is obtained.

References

Abe R, Kamiya N and Matsuda M 1974 *Ferroelectrics* **8** 557–8
Baumgartner H B 1951 *Helv. Phys. Acta* **24** 326–9
Březina B, Janoušek V, Mareček V and Smutný F 1970 *Proc. Europ. Meet. Ferroelectricity* ed. H E Müser and J Petersson (Stuttgart: Wissenshaftliche Verlagsgesellschaft) pp 369–73
Fousek J 1987 *Electro-optic and Photorefractive Materials* ed. P Günter (Berlin: Springer) pp 18–34
Fousek J, Cross L E and Seely K 1970 *Ferroelectrics* **1** 63–70
Fousek J and Petzelt J 1979 *Phys. Status Solidi* a **55** 11–40
Gerbaux X, Hadni A, Pierron J and Messaadi S 1985 *Int. J. Infrared Millimeter Waves* **6** 131–40
Günter P 1976 *Electro-Optics/Laser* ed. H G Jerrard (Guildford, Surrey: IPC Science and Technology Press) pp 121–30
Kay M I 1978 *Ferroelectrics* **19** 159–64
Khaller K E, Khaav A A, Novik V K and Gavrilova N D 1988 *Sov. Phys.–Solid State* **30** 47–50
Maeda M and Ikeda T 1977 *J. Phys. Soc. Japan* **42** 1931–6
Matthias B T and Hulm J K 1951 *Phys. Rev.* **82** 108–9

Novik V K, Drozhdin S N and Gavrilova N D 1982 *Sov. Phys.–Solid State* **24** 893–5
Pavel M, Fousková A, Holakovský J and Březina B 1988 *Czech. J. Phys.* B **38** 314–20
Sawada A, Udagawa M and Nakamura T 1977 *Phys. Rev. Lett.* **39** 829–32
Sawaguchi E and Cross L E 1971 *Ferroelectrics* **2** 37–46
—— 1972 *IEEE Trans. Sonics Ultrasonics* **SU-19** 327–32
Volkov A A, Goncharov Yu G, Kozlov G V, Petzelt J, Fousek J and Březina B 1986 *Sov. Phys.–Solid State* **28** 1794–5